Microchim Acta (2017) 184:4563–4569
DOI 10.1007/s00604-017-2517-4

SHORT COMMUNICATION

An antibacterial microfluidic system with fish gill structure for the detection of *Staphylococcus* via enzymatic reaction on a chromatic polydiacetylene material caused by lysostaphin

Huisoo Jang[1,2] · **Palan Lee**[1,2] · **Seokjae Kim**[1,2] · **Sun Min Kim**[2,3] · **Tae-Joon Jeon**[1,2]

Received: 17 July 2017 / Accepted: 10 September 2017 / Published online: 18 September 2017

Abstract The authors describe a microfluidic system functionalized with a chromatic nanomaterial (polydiacetylene; PDA) and conjugated to the antimicrobial enzyme lysostaphin (LST) as a means for specific detection of *Staphylococcus* pathogens and to simultaneously perform antimicrobial functions. The LST-loaded PDA vesicles were deposited in a fish gill-like structure on the inner surface of the microchannels. They undergo a color transition from blue to red and enhancement of fluorescence under external mechanical stimulus that is caused by the interaction between *Staphylococcus* and LST which has antimicrobial activity against *Staphylococcus*. Due to its fish gill-mimicking structure, the PDA coated channel has a high surface-to-volume ratio, and this maximizes the binding efficiency between *Staphylococcus* suspended in the fluid and the LST-PDA coating on the microchannels. Consequently, >80% of the *Staphylococcus* are eliminated in the channels within a short reaction time. As a result, the LST-PDA-coated channel surfaces undergoes color change from blue to red, and red fluorescence pops up. In contrast, no enzymatic reaction and no color transition is observed when an *E. coli* suspension is applied. The results show that this multifunctional microfluidic system can specifically detect, and can exert an antimicrobial effect on, *Staphylococcus*.

Keywords Multifunctional microfluidic system · Biomimic structure · Chromatic transition · Pathogen detection · Antimicrobial activity · Polydiacetylene (PDA) vesicle · Biosensor · Biofilm · Liposome

Introduction

Microfluidic systems that handle a small amount of fluid in microchannel are an emerging tool used in various engineering fields, such as chemical engineering, biomedical engineering, and mechanical engineering [1]. The miniaturized dimensions and high surface-to-volume ratios of microfluidic devices enable cost-effective, biosensing applications with high sensitivity and selectivity [2, 3]. Thus, the research and development of microfluidic systems is active and ongoing [4].

Of particular interest, microfluidic devices for biomedical applications take advantage of the unique functions of biological molecules by immobilizing proteins on the channel surfaces [5]. For instance microfluidic systems with antibody that is a target-specific biomolecule are enabling highly sensitive diagnosis and sensing of target molecules with few microliter of biomarker due to their rapid mass transfer in microfluidic channels [6]. As another example, microfluidic systems with enzyme provide the most suitable small-scale reaction platforms for synthesizing DNA or RNA at high efficiency [7].

More interestingly, microfluidic applications with biomolecules were not limited to single-function devices where one

Huisoo Jang, Palan Lee and Seokjae Kim contributed equally to this work.

Electronic supplementary material The online version of this article (https://doi.org/10.1007/s00604-017-2517-4) contains supplementary material, which is available to authorized users.

✉ Sun Min Kim
sunmk@inha.ac.kr

✉ Tae-Joon Jeon
tjjeon@inha.ac.kr

[1] Department of Biological Engineering, Inha University 22212, Incheon, South Korea

[2] Biohybrid Systems Research Center (BSRC), Inha University 22212, Incheon, South Korea

[3] Department of Mechanical Engineering, Inha University 22212, Incheon, South Korea

type of antibody or enzyme is immobilized but also functional nanomaterials were added to improve the functions of biomolecules [8]. For example, fluorescent nanoparticles were conjugated to antibodies to improve the sensitivity and reaction activity of immunoassays [9, 10]. Similarly, in an enzyme microreactor, nanoparticles were employed to indicate enzymic reactions in situ [11]. Another example of a multifunctional microfluidic device is a reusable enzyme reactor developed using nanoparticle and enzyme interactions [12], thereby expanding applications of microfluidic systems by providing additional functions to biomolecules immobilized in microfluidic channels.

This report describes a multifunctional microfluidic system with an enzyme-based antibacterial function that can also detect bacteria via sensor materials coupled to the enzyme. Lysostaphin (LST) is an enzyme with antibacterial activity against *Staphylococcus*, which causes a cardiac disorder, a nerve disorder, a respiratory disease, hematosepsis and food poisoning [13, 14]. LST was then conjugated to the surface of polydiacetylene (PDA) vesicles that have a color transition from blue to red and fluoresce when physical or chemical stimuli are applied to the vesicles [15]. To obtain microfluidic channels with both antibacterial and detection functions, the channel surface was conjugated to PDA vesicles and then LST was functionalized on the surface of the PDA vesicles. Furthermore, to maximize the reaction efficiency between the bacteria and the channel surface, our channel structure was inspired by the comb-like fish gill that has a high efficiency in exchange of gas and biomolecules when water passes through the structure [16–18]. As a result, we created a multifunctional microfluidic system capable of simultaneous detection and elimination of bacteria in a single device. Our multifunctional channels are applicable to biomedical devices and diagnostic applications, including intravenous (IV) lines, surgical tubing, point-of-care testing, and other applications.

Materials and methods

Chemicals

LST (L9043), 10,12-pentacosadiynoic acid (PCDA) (76492), propylene glycol monomethyl ether acetate (PGMEA) (484431) and N-hydroxysuccinimide (NHS) (130672) were purchased from Sigma-Aldrich (St. Louis, MO, USA) (http://www.sigmaaldrich.com). 3-Aminopropyl triethoxysilane (APTES, 98%) (A10668), 1-(3-dimethylaminopropyl)-3-ethylcarbodiimide hydrochloride (EDC) (A10807) and 99% HEPES (A14777) were purchased from Alfa Aesar (Ward Hill, MA, USA) (http://www.alfa.com). APTES (5% *v*/v) and HEPES buffer (5 mM pH 7.5) were prepared with deionized water (Direct-Q3, >18. 0 MΩ·cm at 25 °C) from Merck Millipore (Billerica, MA, USA) (http://www.merckmillipore.com). Polydimethylsiloxane (PDMS) prepolymer and curing agent (Sylgard 184) were purchased from Dow Corning (Midland, MI, USA) (http://www.dowcorning.com), and 1,2-dimyristoyl-sn-glycero-3-phosphocholine (DMPC) (850345P) was obtained from Avanti Polar Lipids, (Alabaster, AL, USA) (http://www.avantilipids.com). SU-8 2150 from Microchem (Newton, MA, USA) (http://www.microchem.com) was used as negative photoresist, and BSA (Albumin fraction V heat shock isolation pH 7.0) from Bio Basic, Inc. (Markham, Ontario L3R 8 T4, Canada) (http://www.biobasic.com) was used as blocking buffer. Beef extract (0114) and Peptone (211677) were purchased from Amresco (Solon, OH, USA) (http://www.amresco-inc.com) and BD (San Diego, CA, USA) (http://www.bd.com), respectively. Except for the APTES solution, HEPES buffer and culture media, all solutions were prepared with 5 mM HEPES buffer.

Fabrication of gill-like microfluidic channels

The microchannels were fabricated by a soft lithography process [19]. First, we coated SU-8 2050 on a silicon wafer at 200 μm thick using a spin coater (SP-60P, Shinu Mst, Korea). The microchannel patterned film mask covered the SU-8 above the silicon wafer, and UV light (365 nm of wavelength) was irradiated through the patterned area of the film mask to polymerize specific regions. The microchannel patterned mold was completed after the removal of unpolymerized SU-8 using PGMEA as the developer. A PDMS solution of prepolymer and curing agent at a 10 to 1 ratio (*w*/w) was poured onto the microchannel patterned mold, and bubbles were removed using a vacuum pump. The PDMS solution was cured in a convection oven at 60 °C for 4 h. Cured PDMS was detached from the mold and punched by a micro-punch to make inlet and outlet holes for fluid injection. The PDMS replica was attached to the slide glass by a plasma bonding method immediately prior to the experiment. The film mask was designed to mimic fish gill structure by using AutoCAD software (Autodesk Inc., USA) (http://www.autodesk.com). The oval-shaped pillars in the microchannel were constructed at 30, 45 and 60°.

PDA vesicle preparation

PDA vesicles were prepared by a previously reported method [20]. First, PCDA and DMPC in a 4 to 1 ratio were dissolved in chloroform in a glass vial. Lipid-dissolved chloroform was evaporated by a gentle stream of argon gas, and the residual solvent was removed in a vacuum. HEPES buffer (5 mM, pH 7.5) was added to obtain a final lipid concentration of 2 mM. The vial was placed in an 80 °C water bath for 15 min. The solution was sonicated using a probe sonicator

(VCX 500, Sonics, USA) (http://www.sonics.com) at 27% power for 15 min to disperse the PDA vesicles. This PDA solution was filtered with a 0.8 μm syringe filter and stored at 4 °C overnight to stabilize the PDA solution.

Immobilization of PDA vesicles and lysostaphin in the microfluidic channel

PDA vesicles and LST were sequentially conjugated to the surface of the microchannels through an EDC/NHS coupled reaction [21, 22]. First, the PDA vesicles were activated by 2 mM of EDC and NHS for 2 h at room temperature on a rotary shaker. After the reaction, unreacted EDC and NHS were removed by centrifugation at 14,000 g for 10 min using a 3 kDa centrifugal filter. Activated PDA vesicles were conjugated to the surface of a microchannel functionalized with an amine through APTES. Next, 5% APTES solution (*v*/v) was immediately injected into the microfluidic channel after the device was sealed by plasma bonding for 2 min. Activated PDA vesicles were then injected into the microchannels and placed at room temperature for 2 h for the conjugation reaction. To conjugate LST onto the surface of the PDA vesicles in the microchannels, HEPES buffer containing LST (200 μg·mL^{-1}) was injected into the microchannels, and the device was placed at room temperature for 2 h (Fig. 1a). After the reaction, the microchannels were washed with HEPES buffer to remove extra LST. BSA solution (2 mg·mL^{-1}) was injected to mask the unreacted surface of PDA vesicles in the microchannels, and the device was washed with HEPES buffer. The conjugated PDA vesicles were then irradiated with 254 nm UV light for 3 min to induce a color transition to blue.

Flowing a bacterial solution through a microfluidic channel

S. epidermidis (ATCC 14990), the target bacterium, was obtained from the Korean Culture Center of Microorganisms (KCCM) (http://www.kccm.or.kr). These bacteria were cultivated in a culture medium containing 3 g·L^{-1} beef extract and 5 g·L^{-1} of peptone at pH 7.0 and 37 °C overnight in a shaking incubator at 127 rpm to concentration of 1.8×10^9 cfu·mL^{-1}. *E. coli*, the negative control, was also cultivated in LB broth under the same conditions to concentration of 1.01×10^9 cfu·mL^{-1}. In the antibacterial experiment, antibacterial activity was determined by the turbidimetric enzyme activity assay with slight modification [23]. Each bacterial solution was injected into the microchannels at a flow rate of 30 μL·min^{-1} at room temperature. To determine the antibacterial activity, the OD_{600} value was measured using a spectrophotometer (Genesis 10UV, Thermo Scientific, USA) (http://www.thermofisher.com). After the solution was injected, 2 mL of bacterial solution from the microchannel was collected and analyzed by spectrophotometer (Genesis 10UV, Thermo Scientific, USA) (http://www.thermofisher.com) to compare the OD_{600} value with the initial OD_{600} value before injection into the microchannel.

Microscopy experiment

Microchannels were observed by an inverted microscope (Eclipse TI-U, Nikon, Japan) (http://www.nikon.com). To take fluorescent images, a metal halide lamp (C-HGFI, Nikon, Japan) and green fluorescent filter (G-2A, Nikon, Japan) were applied to expose specific light at 510–560 nm in wavelength. The obtained images were further analyzed using Image J Software (NIH, Bethesda, MD) (https://imagej.nih.gov/ij/download.html) to measure fluorescence intensity for quantitative analysis.

Results and discussion

Microfluidic channel inspired by a fish gill

We have devised a microfluidic channel structure inspired by a fish gill that has a large surface-to-volume ratio to maximize the reaction between bacteria and the channel surfaces where LST-PDA vesicles were coated (Fig. S1). The fish gill has a comb-like lamellar structure in the constricted area, which has a high gas exchange efficiency when water passes through the structure [16–18]. We fabricated pillars mimicking the comb-like lamellae structure on the interior of the microfluidic channels; thus, the bacteria reacted more effectively with the LST-PDA conjugated on the surfaces of the pillars and channels. The height, width and length of the channels were 200 μm, 1 mm and 2 cm, respectively. The inclusion of pillars 500 μm in length and 100 μm in width within the channel made the surface-to-volume ratio three times higher than that of a channel without the pillars.

Immobilization of PDA vesicles on the interior of the channel

To provide the two functions of antibacterial activity and detection, we coated both the pillar and channel surfaces with PDA vesicles and then conjugated LST onto the surface of the PDA vesicles. Diacetylene monomers form self-assembled vesicles in aqueous solution, and subsequent UV illumination polymerizes the diacetylene monomers, creating PDA vesicles. After polymerization, the blue PDA vesicles undergo a color transition to red and fluoresce enhancement in response to external stimuli, such as mechanical stress [24]. The mechanical stress applied to the PDA vesicles induces distortion in polymerized network of the PDA vesicles, which widens a HOMO-LUMO energy band gap, resulting in the change of

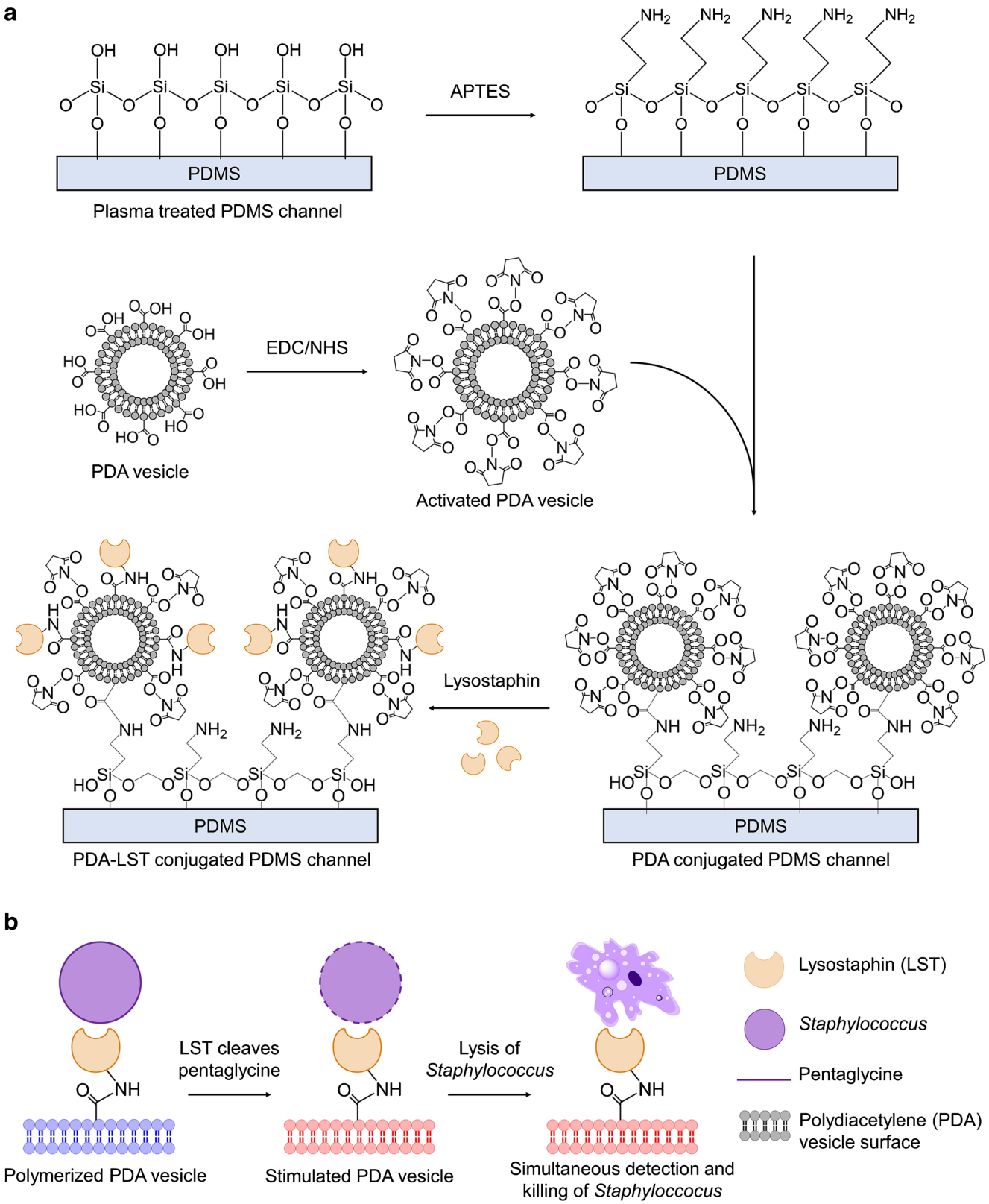

Fig. 1 Schematic illustration of the entire reaction on the microfluidic surfaces: **a** Fabrication of PDA-LST-conjugated PDMS channel. PDA vesicles can be activated using EDC/NHS chemistry. Amine groups on the PDMS surface and activated PDA vesicles were bound through the EDC/NHS reaction. LST, an amine-rich enzyme, can also be coupled to activated PDA using the same chemistry. **b** The antibacterial reaction of LST induces a color transition of the PDA vesicles. LST lysed *Staphylococcus* by cleaving pentaglycine in their cell walls, and the mechanical stress during the reaction between LST and bacteria made the PDA vesicles change color from blue to red

optical property of the PDA vesicles [25]. In this study, the color change and fluorescence enhancement occurred in response to the mechanical stress of antibacterial reaction between LST and *S. epidermidis* (Fig. 1b).

The PDA vesicles used for our experiments ranged from 100 to 200 nm in size. DMPC was added among the diacetylene monomers at a ratio of 1:4 to increase the sensitivity of the color transition of PDA vesicles [26]. We conjugated PDA vesicles to the surface of the pillars and channels through an EDC/NHS reaction between the carboxyl end of diacetylene and the amine-rich surface of PDMS treated by oxygen plasma and APTES. We observed aggregation of the PDA vesicles when a high concentration of reaction mixture was used; thus, 2 mM PDA vesicles and NHS and EDC solutions were used to prevent aggregation. To verify the conjugation of PDA vesicles on the surfaces, a color change was induced by flowing 1 N NaOH solution through the channels after UV illumination for 3 min, and fluorescence was observed along the surfaces of the channels (Fig. S2).

Antibacterial activity by LST

LST is an enzyme that cleaves the pentaglycine cross-bridge in the cell wall of certain *Staphylococci* [12]. LST-PDA conjugated onto the channel and pillar surface lyses *Staphylococci*, whose cell wall is composed of a pentaglycine cross-bridge, via cell wall damage. *S. epidermidis* at a concentration of 1.8×10^9 cfu·mL^{-1} after 24 h of incubation flowed through the channel. The OD_{600} was measured to compare the death rate before and after the bacteria flowed through the channels. The OD value dropped by 80 ± 8.32 (SD)% when *S. epidermidis* was flowed through the PDA-LST-conjugated channel, whereas almost no change was observed in the negative control lacking LST. Moreover, *E. coli* remained intact when flowed through LST-PDA-coated channels (Fig. 2) [27].

Our data show promising results because previous work with antibacterial solutions in a stagnant state showed a death rate of 70–80%; in contrast, in our system, bacteria were continuously flowed through the channel with a limited retention time and exposure to LST prior to flowing out of the channels but had a similar death rate [28–30]. Our system with continuous flow in the microchannels can be used for more practical applications, such as IV injection lines, tubing, or pipelines.

To investigate the effect of angles of the pillar, we made pillars at various angles, 30, 45 and 60°, to the flow direction. Of the three angles, 60° led to the largest decreases in OD of 88.3%, and 30° and 45° led to decreases of 83.9% and 86.6%, respectively (Fig. S3); this finding is attributed to the ratio of the cross-sectional area of the pillars within the channels. A higher cross-sectional area will create turbulent flow in the channels, resulting in higher mixing efficiency and antibacterial activity on the surface of the channels [31].

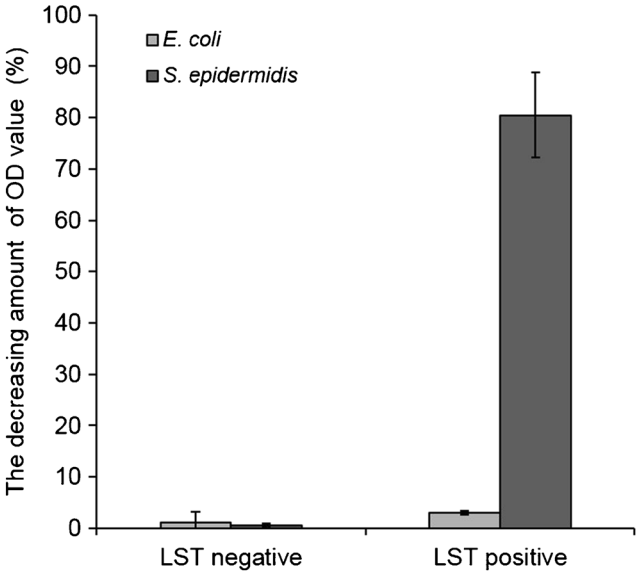

Fig. 2 The OD value decreases as the reaction between LST and *S. epidermidis* increases. With no LST, the OD values remained the same before and after each bacterial suspension flowed through the channels. The OD values changed considerably when *S. epidermidis* flowed through the PDA-LST-conjugated channels. The PDA-LST-conjugated channel can kill *S. epidermidis* and has specificity against *S. epidermidis*. Data (n = 5) were collected with five different sets of devices

The specificity of LST to *S. epidermidis* was shown by using *E. coli* as a control. Since *E. coli* does not have pentaglycine in the cell wall, *E. coli* should not react with LST, and the OD values remained the same before and after flowing through the channel. Fig. 2 shows that the LST-coated channels reacted specifically with *S. epidermidis* but not with *E. coli*. In addition, the channels with bare surfaces also did not demonstrate activity against either *E. coli* or *S. epidermidis*.

Detection of *S. epidermidis* using the chromatic transition of PDA

To observe the chromatic transitions of channel surfaces coated with PDA-LST on reaction with *S. epidermidis*, the channels were viewed under a fluorescence microscope. A notable color change occurred, as shown in Fig. 3c, whereas no or little color change was observed in Fig. 3a and b when *E. coli* was flowing on the PDA-LST-coated surface and *S. epidermidis* was flowing on the PDA only surface, respectively. The slight change found in Fig. 3b was due to some non-specific binding to unblocked PDA surfaces attributed to the culture medium. Further quantitative analysis performed using Image J indicated that the fluorescence intensity in Fig. 3c was almost five times as high as that of the other control experiment (two-tailed t-test, p-value <0.01) as shown in Fig. 3d, showing the specificity of color changes to

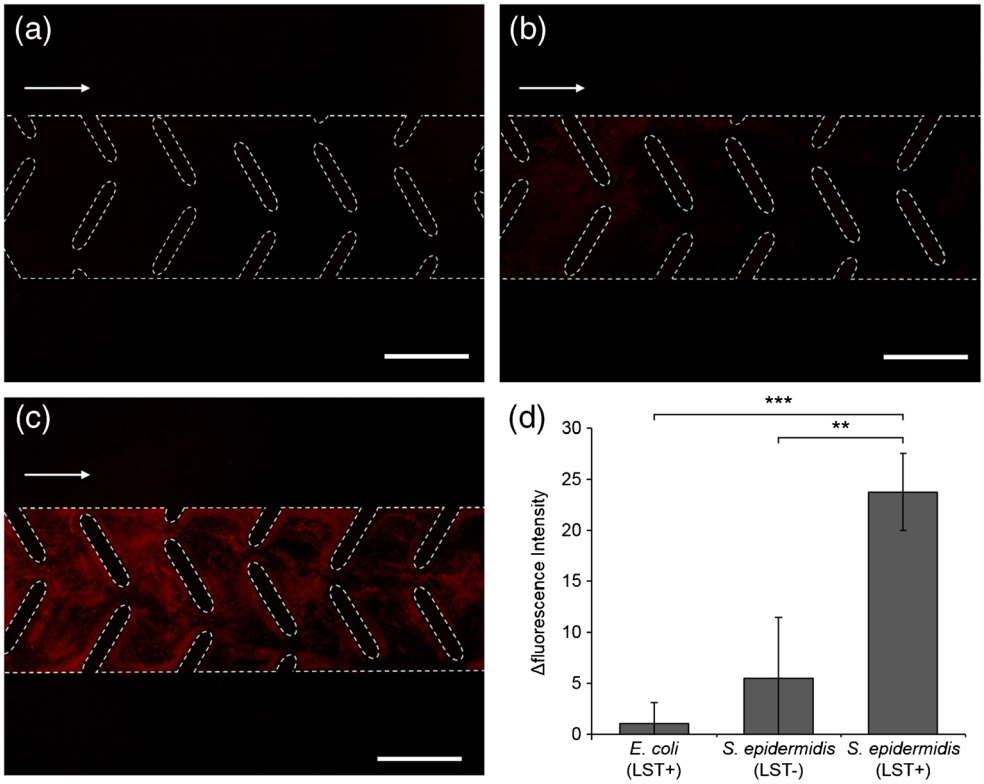

Fig. 3 Chromatic transitions on the microfluidic channels. When *E. coli* flowed through (**a**) an LST-positive channel (PDA-conjugated channel), no noticeable change in fluorescence intensity was observed. When *S. epidermidis* flowed through the channels, the channel surfaces with bare PDA vesicles (**b**) exhibited slight color changes due to non-specific interactions, but the changes were less than those of (**c**) the LST-positive channel. Dotted lines and arrows show the boundary of the channels and the direction of bacterial flow, respectively. Scale bar = 500 μm. (**d**) The amount of change in fluorescence intensity depended on the specific reaction between LST and *S. epidermidis*. Data ($n = 6$) were collected from six different devices. Two-tailed t-test. (**) and (***) indicate $p < 0.01$ and $p < 0.001$, respectively

S. epidermidis. The color changes were specifically attributed to the reaction between LST and *Staphylococcus*.

Using *E. coli*, we showed the specificity of the channel to *S. epidermidis*. Only when *S. epidermidis* flowed through, did the PDA- and LST-conjugated channel exhibit the color transition of PDA vesicles (Fig. 3c). The channels with *E. coli* (Fig. 3a) or without LST (Fig. 3b) did not undergo the transition. Even when LST was present in the channel, the fluorescence intensity of PDA vesicles with *S. epidermidis* was more than 20 times higher than that of the channels with *E. coli* (two-tailed t-test, p-value <0.001) as shown in Fig. 3d. These results indicate that the color transition of PDA vesicles was induced by the reaction between LST and *S. epidermidis* and that the channel has specificity for *S. epidermidis*. However, correlation of fluorescence intensity and bacteria concentration was not further analyzed because the amount of chromatic PDA vesicles coated on the channels was not enough to differentiate fluorescence intensities. To improve the sensitivity issue, we can have layer-by-layer coatings of sensing materials or use other chromatic materials, such as quantum dots, that have higher light/fluorescence intensity.

Conclusions

In this study, we developed a microfluidic system that enables chromatic detection of *S. epidermidis* while simultaneously providing antibacterial activity in microfluidic channels coated with LST-conjugated PDA vesicles. Furthermore, we mimicked the fish gill structure to obtain a high surface-to-volume ratio and increase the reaction efficiency between *S. epidermidis* and the microfluidic surfaces. The results showed the high efficiency of the antibacterial activity compared with the previous work with suspended LST solution, and the simultaneous, specific reaction with *S. epidermidis* that enabled the chromatic detection of *S. epidermidis*. Our system can also be modified using different enzymes or antibodies for the purpose of simultaneous detection and elimination of bacteria or fungi present in solution. In addition, the methods presented here should be applicable to any channel surfaces with functional groups where chemically modifiable. Although this system offers multi-functions to channel surfaces, potentially applicable to clinical settings, the detection limit of this system can be an issue. However, the multifunctional system and its applicability to any type of channels are still beneficial as compared to previous work (Table S1). Therefore, once sensitivity of the system is improved, the microfluidic channels shown in this work can be widely used not only in biomedical devices, such as for the diagnosis of pathogens or prevention of IV line contamination, but also in industrial applications, such as pipelines in plants and real-time detection and elimination of pathogens for safe tubing.

Acknowledgements This work was supported by an Inha University Research Grant.

Compliance with ethical standards The author(s) declare that they have no competing interests.

References

1. Whitesides GM (2006) The origins and the future of microfluidics. Nature 442:368–373. https://doi.org/10.1038/nature05058
2. Mark D, Haeberle S, Roth G et al (2010) Microfluidic lab-on-a-chip platforms: requirements, characteristics and applications. Chem Soc Rev 39:1153. https://doi.org/10.1039/b820557b
3. Haeberle S, Mark D, von Stetten F, Zengerle R (2012) Microfluidic platforms for lab-on-a-chip applications. Microsyst Nanotechnol 853–895. https://doi.org/10.1007/978-3-642-18293-8_22
4. Chen C, Mehl BT, Munshi AS et al (2016) 3D-printed microfluidic devices: fabrication, advantages and limitations-a mini review. Anal Methods 8:6005–6012. https://doi.org/10.1039/c6ay01671e
5. Kim D, Herr AE (2013) Protein immobilization techniques for microfluidic assays. Biomicrofluidics 7(4):41501. https://doi.org/10.1063/1.4816934
6. Chen W, Huang N-T, Li X et al (2013) Emerging microfluidic tools for functional cellular immunophenotyping: a new potential paradigm for immune status characterization. Front Oncol 3:98. https://doi.org/10.3389/fonc.2013.00098
7. Asanomi Y, Yamaguchi H, Miyazaki M, Maeda H (2011) Enzyme-immobilized microfluidic process reactors. Molecules 16:6041–6059. https://doi.org/10.3390/molecules16076041
8. Hu C, Yue W, Yang M (2013) Nanoparticle-based signal generation and amplification in microfluidic devices for bioanalysis. Analyst 138:6709–6720. https://doi.org/10.1039/c3an01321a
9. Chen X, Cui D, Li H et al (2010) Microfluidics-based immunoassays by using an integrated fluorescence detection system. Microsyst Technol 16:2049–2055. https://doi.org/10.1007/s00542-010-1150-5
10. Ryu G, Huang J, Hofmann O et al (2011) Highly sensitive fluorescence detection system for microfluidic lab-on-a-chip. Lab Chip 11:1664–1670. https://doi.org/10.1039/c0lc00586j
11. Kerby MB, Legge RS, Tripathi A (2006) Measurements of kinetic parameters in a microfluidic reactor. Anal Chem 78:8273–8280. https://doi.org/10.1021/ac061189l
12. Ender F, Weiser D, Poppe L (2016) Microfluidic multiple chamber chip reactor filled with enzyme-coated magnetic nanoparticles. In: Stoytcheva M (ed) Lab-on-a-chip fabrication and application. InTech. http://doi.org/10.5772/62512
13. Wu JA, Kusuma C, Mond JJ, Kokai-Kun JF (2003) Lysostaphin disrupts Staphylococcus aureus and Staphylococcus epidermidis biofilms on artificial surfaces. Antimicrob Agents Chemother 47(11):3407–3414. https://doi.org/10.1128/AAC.47.11.3407-3414.2003
14. Grundmann H, Aires-de-Sousa M, Boyce J, Tiemersma E (2006) Emergence and resurgence of meticillin-resistant Staphylococcus aureus as a public-health threat. Lancet 368:874–885. https://doi.org/10.1016/S0140-6736(06)68853-3
15. Díaz Nafría JM, Zimmermann RE (2013) Emergence and evolution of meaning. TripleC 11:13–35. https://doi.org/10.1007/128
16. Nilsson GE, Dymowska A, Stecyk JAW (2012) Respiratory physiology & neurobiology new insights into the plasticity of gill structure. Respir Physiol Neurobiol 184:214–222. https://doi.org/10.1016/j.resp.2012.07.012
17. Evans DH, Piermarini PM, Choe KP (2005) The multifunctional fish gill: dominant site of gas exchange, osmoregulation, acid-base regulation, and excretion of nitrogenous waste. Physiol Rev 85:97–177. https://doi.org/10.1152/physrev.00050.2003
18. Wilson JM, Laurent P (2002) Fish gill morphology: inside out. J Exp Zool 293:192–213. https://doi.org/10.1002/jez.10124
19. Xia YN, Whitesides GM (1998) Soft lithography. Annu Rev Mater Sci 28:153–184. https://doi.org/10.1146/annurev.matsci.28.1.153
20. Yong H, Hoon S, June D, et al (2004) Micropatterning of diacetylenic liposomes on glass surfaces 24:157–161. doi:https://doi.org/10.1016/j.msec.2003.09.067
21. Dewi MR, Laufersky G, Nann T (2015) Selective assembly of Au-Fe_3O_4 nanoparticle hetero-dimers. Microchim Acta 182:2293–2298. https://doi.org/10.1007/s00604-015-1571-z
22. Su YL (2005) Assembly of polydiacetylene vesicles on solid substrates. J Colloid Interface Sci 292:271–276. https://doi.org/10.1016/j.jcis.2005.05.049
23. Satishkumar R, Sankar S, Yurko Y et al (2011) Evaluation of the antimicrobial activity of lysostaphin-coated hernia repair meshes. Antimicrob Agents Chemother 55:4379–4385. https://doi.org/10.1128/AAC.01056-10
24. Jung YK, Kim TW, Park HG, Soh HT (2010) Specific colorimetric detection of proteins using bidentate aptamer-conjugated polydiacetylene (PDA) liposomes. Adv Funct Mater 20:3092–3097. https://doi.org/10.1002/adfm.201001008
25. Charoenthai N, Pattanatornchai T, Wacharasindhu S (2011) Roles of head group architecture and side chain length on colorimetric response of polydiacetylene vesicles to temperature, ethanol and pH. J Colloid Interface Sci 360:565–573. https://doi.org/10.1016/j.jcis.2011.04.109
26. Su YL, Li JR, Jiang L (2004) Chromatic immunoassay based on polydiacetylene vesicles. Colloids Surf B: Biointerfaces 38:29–33. https://doi.org/10.1016/j.colsurfb.2004.08.010
27. Walsh S, Shah A, Mond J (2003) Improved pharmacokinetics and reduced antibody reactivity of lysostaphin conjugated to polyethylene glycol. Antimicrob Agents Chemother 47:554–558. https://doi.org/10.1128/AAC.47.2.554-558.2003
28. Yeroslavsky G, Girshevitz O, Foster-Frey J et al (2015) Antibacterial and antibiofilm surfaces through polydopamine-assisted immobilization of lysostaphin as an antibacterial enzyme. Langmuir 31:1064–1073. https://doi.org/10.1021/la503911m
29. Desbois AP, Lang S, Gemmell CG, Coote PJ (2010) Surface disinfection properties of the combination of an antimicrobial peptide, ranalexin, with an endopeptidase, lysostaphin, against methicillin-resistant Staphylococcus aureus (MRSA). J Appl Microbiol 108:723–730. https://doi.org/10.1111/j.1365-2672.2009.04472.x
30. Pangule RC, Brooks SJ, Dinu CZ et al (2010) Antistaphylococcal nanocomposite films based on enzyme-nanotube conjugates. ACS Nano 4:3993–4000. https://doi.org/10.1021/nn100932t
31. Stoecklein D, Wu C-Y, Owsley K et al (2014) Micropillar sequence designs for fundamental inertial flow transformations. Lab Chip 14:4197–4204. https://doi.org/10.1039/C4LC00653D